

**Letter**

# Photoelectron circular dichroism observed in the above-threshold ionization signal from chiral molecules with femtosecond laser pulses

Christian Lux<sup>1</sup>, Arne Senftleben<sup>1</sup>, Cristian Sarpe<sup>1</sup>,  
Matthias Wollenhaupt<sup>2</sup> and Thomas Baumert<sup>1</sup>

<sup>1</sup>Institut für Physik und CINSA, Universität Kassel, Heinrich-Plett-Straße 40, D-34132 Kassel, Germany

<sup>2</sup>Institut für Physik, Carl von Ossietzky Universität Oldenburg, Carl-von-Ossietzky-Straße 9-11, D-26129 Oldenburg, Germany

E-mail: [tbaumert@uni-kassel.de](mailto:tbaumert@uni-kassel.de)

Received 4 September 2015, revised 30 October 2015

Accepted for publication 17 November 2015


Published 22 December 2015



CrossMark

**Abstract**

Photoelectron circular dichroism is investigated experimentally as a function of the number of absorbed circularly polarized photons. Three structurally different chiral molecules yet showing similar absorption spectra are studied. They are isotropically distributed in the gas phase and ionized with femtosecond laser pulses. We measure and analyze the photoelectron angular distribution of threshold electrons ionized with three photons and compare them to those of above-threshold (ATI) electrons ionized with four photons. Additionally to an increase in high even order Legendre polynomials the coefficients of the high odd order Legendre polynomials rise with increasing photon number. Consequently, the ATI electrons also carry the chirality signature. All investigated chiral molecules reveal an individual set of coefficients for the threshold and ATI signatures despite their similarities in chemical structure. The presented data set can serve as a guideline for theoretical modeling of the interaction of circularly polarized light with chiral molecules in the multiphoton regime.

 Online supplementary data available from [stacks.iop.org/JPB/49/02LT01/mmedia](https://stacks.iop.org/JPB/49/02LT01/mmedia)

Keywords: PECD, chirality, multiphoton, ATI

(Some figures may appear in colour only in the online journal)

The development of quantum physics rests significantly on Albert Einstein's theory of the photoelectric effect [1]. The important role of the photoelectric effect in basic research was underscored by the 1981 Nobelprize in physics awarded to Kai Siegbahn for 'his contribution to the development of high-resolution electron spectroscopy'. Up to now, photoelectron spectroscopy has remained one of the central techniques to unravel new types of light-matter interaction due to its sensitivity both to electronic structure and its dynamics in

atoms, molecules, surfaces and solids [2–4]. An important extension of the original approach was to add angular resolution [5]. With the advent of intense laser pulses the photoelectric effect could be studied in much stronger fields giving rise to multi-photon ionization [6, 7]. In this regime, photoelectron spectroscopy unraveled the mechanism of above-threshold ionization (ATI) [8], where more photons are absorbed than necessary to overcome the ionization potential. Further ATI investigations range from first studies of high

order even Legendre polynomials in the corresponding photoelectron angular distribution (PAD) of ATI from atoms [9] to the influence of molecular vibrational wave-packet motion onto the ATI electrons in a femtosecond time-resolved experiment [10]. In addition, channel resolved ATI was recently developed to resolve the multiple electronic continuum channels in strong field ionization of polyatomic molecules [11].

In the last 15 years angle-resolved photoelectron spectroscopy has been increasingly applied to ionization of randomly oriented enantiomers of chiral molecules with circularly polarized light. There, the PAD shows a distinctive asymmetry with respect to the light propagation direction. The asymmetry changes its direction dependent on the handedness of the enantiomer and the helicity of the ionizing light. This circular dichroism (CD) effect in the differential photoionization cross section was theoretically predicted by Ritchie [12] using an electric dipole approximation. Because of this electric dipole nature, the photoelectron circular dichroism (PECD) can be several orders of magnitude larger than conventionally measured CD. Therefore, PECD delivers a promising tool for spectroscopic studies of chiral species in the gas phase and shows high potential for analytical applications. With the help of one-photon vacuum ultraviolet (VUV) synchrotron radiation, PECD was investigated on many small chiral molecules in the detection of angular resolved photoelectron emission [13, 14]. These measurements have later been extended to the application of the velocity-map imaging (VMI) technique [15]. The synchrotron radiation based PECD results have been reviewed by Powis [16]. Recently, a high harmonic laser source was used to deliver VUV light for a one-photon PECD experiment [17]. The implementation of multiphoton ionization schemes in a table-top laser-based PECD experiment was demonstrated using VMI detection [18, 19] and confirmed with coincidence detection [20]. Present developments also covering multiphoton schemes in PECD measurements have been discussed in a perspective article [21].

When multiphoton ionization with femtosecond pulses is compared to single-photon ionization on randomly oriented chiral molecules, PECD shows contributions from higher order Legendre polynomials [18–20]. This can be rationalized from general considerations: PADs from the ionization of isotropically distributed molecules with linearly or circularly polarized light can be expanded into the cylindrically symmetric Legendre polynomials  $P_l(\Theta)$  and corresponding Legendre coefficients  $c_l$  for a specific ionization channel [2, 22]:

$$P(\Theta) \propto \sum_{l=0}^{l_{\max}} c_l P_l[\cos(\Theta)]. \quad (1)$$

In the cases of left (LCP) or right circularly polarized (RCP) light the Legendre polynomials are cylindrically symmetric around the light propagation direction.  $\Theta$  is the angle measured between this symmetry axis and the ejection direction of the photoelectron. Furthermore, the even

Legendre polynomials are symmetric with respect to the origin of the distribution and the light propagation, and the odd polynomials are antisymmetric with that respect. The number of photons ( $n$ ) in the multiphoton ionization is reflected in the appearing maximum order of the contributing Legendre polynomials. According to Yang's theorem [23] the maximum order should be  $l_{\max} = 2n$  (see Dixit and McKoy [24]).

In one-photon ionization of achiral systems equation (1) reduces to the zeroth and second order Legendre polynomial [2]. Whereas in the case of randomly oriented chiral molecules and circularly polarized single-photon ionization the first odd-order Legendre polynomial ( $P_1$ ) has to be taken into account. Due to parity conservation [25], the corresponding coefficient  $c_1$  changes its sign upon exchanging the handedness of the circularly polarized light or the enantiomer.

PADs containing high-order odd Legendre polynomials—that alter sign by changing the enantiomer or helicity of light—have been recently observed: taking chemically similar molecules from the family of bicyclic ketones, different modulations and amplitudes of the contributing Legendre polynomials have been reported for camphor, fenchone and norcamphor [19]. These stem from resonance enhanced multiphoton ionization (REMPI), where two photons are used to reach an intermediate and one photon is used to ionize out of this intermediate (2 + 1 REMPI). So far there is a lack of a consistent theoretical description of PADs from chiral molecules and therefore also for the PECD in the multiphoton case: field induced polarizability of the intermediate has been used to simulate higher-order polynomials in the PECD after one-photon ionization of camphor out of a resonant intermediate [20]. In another approach higher-order polynomials direct from ground-state multiphoton ionization have been calculated for camphor and fenchone making use of a continuum-state corrected strong-field approximation [26]. Besides producing higher order Legendre polynomials, neither the quantitative nor qualitative agreement with experiments was satisfying. A general nonperturbative method for the theoretical investigation of the angle-resolved multiphoton ionization of polyatomic molecules by intense short differently polarized laser pulses has been developed recently and will be applied to investigate PECD in the multiphoton ionization of bicyclic ketones in the future [27].

In order to provide a further guideline for theoretical development we study PECD as a function of the number of absorbed photons within a consistent dataset. To that end, we performed PECD experiments on camphor, fenchone and norcamphor and retrieved the contributing Legendre polynomials for the threshold photoelectrons, corresponding to the absorption of three photons, and for the first ATI photoelectrons, corresponding to the absorption of four photons.

A detailed description of the experimental set-up, the properties of the investigated molecules together with the corresponding ionization scheme and data evaluation has been reported earlier [19]. In brief, femtosecond laser pulses with a central wavelength of 398 nm and full width at half maximum (FWHM) pulse duration of 25 fs are focused on an effusive gas beam in the interaction region of our VMI

spectrometer. To measure the PECD-effect we use an achromatic quarter-wave plate to generate either left (LCP) or right circularly polarized (RCP) light, where we use the optical convention [28] for assignment. For both polarizations the experimentally determined value of the Stokes  $S_3$  parameter [28] is  $|S_3| = 99\%$ .

At  $7 \mu\text{J}$  pulse energy the peak intensity  $I_0$  in the focus is approx.  $1 \times 10^{13} \text{ W cm}^{-2}$  as verified by measured ponderomotive shifts in Xe [19]. At  $I_0$  a Keldysh  $\gamma$  parameter larger than five is obtained for the molecules studied here with ionization potentials ranging from 8.6 eV to 9.2 eV. Hence, ionization appears in the multiphoton regime. This was confirmed by reducing the intensity in several steps up to half an order of magnitude below  $I_0$ . For all molecules the threshold signal gave the expected multiphoton exponent of about three (between 2.5 and 3.2, consistent with values reported in [19]) and the ATI signal of about four (between 3.4 and 4.2). The resulting three-dimensional PADs, i.e. three-dimensional momentum distributions of the released photoelectrons, are Abel-projected onto an imaging assembly. The propagation direction of the laser is perpendicular to the spectrometer axis ( $x$ -axis) and coplanar to the detector surface which is parallel to the ( $y, z$ )-plane (see figure 1). In the measured PAD images  $I(y, z)$  the  $k$ -vector is always along the positive  $z$ -axis. The PECD-image  $\text{PECD}(y, z)$  is derived for each enantiomer from the measured PAD-images using LCP and RCP, respectively:

$$\text{PECD}(y, z) = I^{\text{LCP}}(y, z) - I^{\text{RCP}}(y, z). \quad (2)$$

In order to visualize the PECD-effect for photoelectrons stemming from different energy channels and with different signal strength, we define the PECD contrast

$$\text{PECD}_{\text{contrast}}(y, z) = \frac{I^{\text{LCP}}(y, z) - I^{\text{RCP}}(y, z)}{I^{\text{LCP}}(y, z) + I^{\text{RCP}}(y, z)}. \quad (3)$$

The photoelectron energy resolution in the presented measurements is better than 80 meV FWHM at an energy of about 0.5 eV and better than 140 meV at 2 eV. The accuracy for the assignment of the energy value is approx.  $\pm 10$  meV in a range of 0.5–1.5 eV and about  $\pm 50$  meV between 2.5 and 3.5 eV.

We studied the PECD in ATI and threshold ionization for the bicyclic ketones camphor, fenchone and norcamphor which are quite similar in mass and structure. All enantiomeric samples possess a constitutional purity of over 98%. The enantiomeric excess (ee) values for (R)-(+)-camphor and (S)-(–)-camphor are  $>98\%$ . (S)-(+)-fenchone has 99.8% ee and (R)-(–)-fenchone 84.0%. The ee of (S)-(+)-norcamphor is  $>95\%$ . The ionization of these molecules proceeds from the highest occupied orbital via a  $2 + 1$  REMPI. Reported vertical IPs are 8.7 eV for camphor, 8.6 eV for fenchone and 9.17 eV for norcamphor. The ionization scheme has been presented earlier [19, 29]. The measured excess energies showed a maximum at 0.52 eV in the case of camphor, at 0.56 eV for fenchone and at 0.23 eV for norcamphor all with a FWHM of approximately 200 meV. This  $2 + 1$  REMPI has

been confirmed by intensity dependent observations [18, 19]. All results hint to an ionization process, where the PECD is originating from photoelectrons stemming directly from the parent molecules before it fragments [18, 19]. Moreover, no significant ponderomotive shifts in the excess energy as well as changes in the PADs have appeared in those intensity variations [19]. Only a small decrease of the PECD-effect with increasing intensity has been observed. These studies and the observed maxima of the excess energies hint to intermediate states acting as dynamic Freeman resonances [30].

For the investigated molecules the PECD contrasts (derived using equation (3)) are presented in figure 1. The different distinctive asymmetries of the known threshold signatures in the photoelectron distributions are clearly visible for camphor, fenchone and norcamphor [18, 19] in the central part of each image. Furthermore, for all enantiomers a second energy channel appears at a larger radius also showing a PECD-effect in the 10% regime. This outer ring is attributed to the first ATI and shows additional structure, most pronounced in the (S)-(+)-norcamphor data: The threshold photoelectrons exhibit significantly non-zero PECD-values along the  $z$ -axis, while the ATI-PECD almost vanishes in forward and backward direction. This observation indicates the additional angular momentum added by the fourth photon which additionally pushes away the maxima and minima from the  $z$ -axis as clearly visible in the presented Abel-inverted data (see lower-right image of figure 1 and supplementary information).

For a further quantification, we concentrate on Abel-inverted data. The Abel-inversion was performed on the measured PAD-images using an adapted pBasex algorithm [19, 31]. From Yang's theorem [23] a decomposition of a PAD resulting from ionization via a four-photon process into four even and four odd components is sufficient. Higher order polynomials were included in the analysis, but these did not contain significant amplitudes in the coefficients. As symmetrical contributions in the measured PECD-images are attributed to residual optical imperfections of our set-up, we concentrate mainly on the appearing antisymmetric contributions in the measured and analyzed data, which are described by the odd order coefficients [19]. As an example, the energy calibrated antisymmetric part of the Abel-inverted PECD-image (see equation (2)) from (S)-(+)-norcamphor is displayed in figure 1 third row, right image. Therein, the signal from the ATI signature has a maximum at approx. 3.4 eV (threshold  $\sim 0.23$  eV) which energetically corresponds to the additional absorption of one 398 nm photon. The ATI-signature of camphor shows up at a maximum of about 3.7 eV (threshold  $\sim 0.52$  eV) and for fenchone at approx. 3.8 eV (threshold  $\sim 0.56$  eV), again consistent with the absorption of an additional photon within the accuracy of our spectrometer.

For the quantification of the measured angular distributions the Legendre coefficients within the FWHM of the threshold and the ATI energy channel were extracted. Those are illustrated up to the 8th order in figure 2 and listed in the Supporting Information together with different graphic representations. For each enantiomer and each energy channel

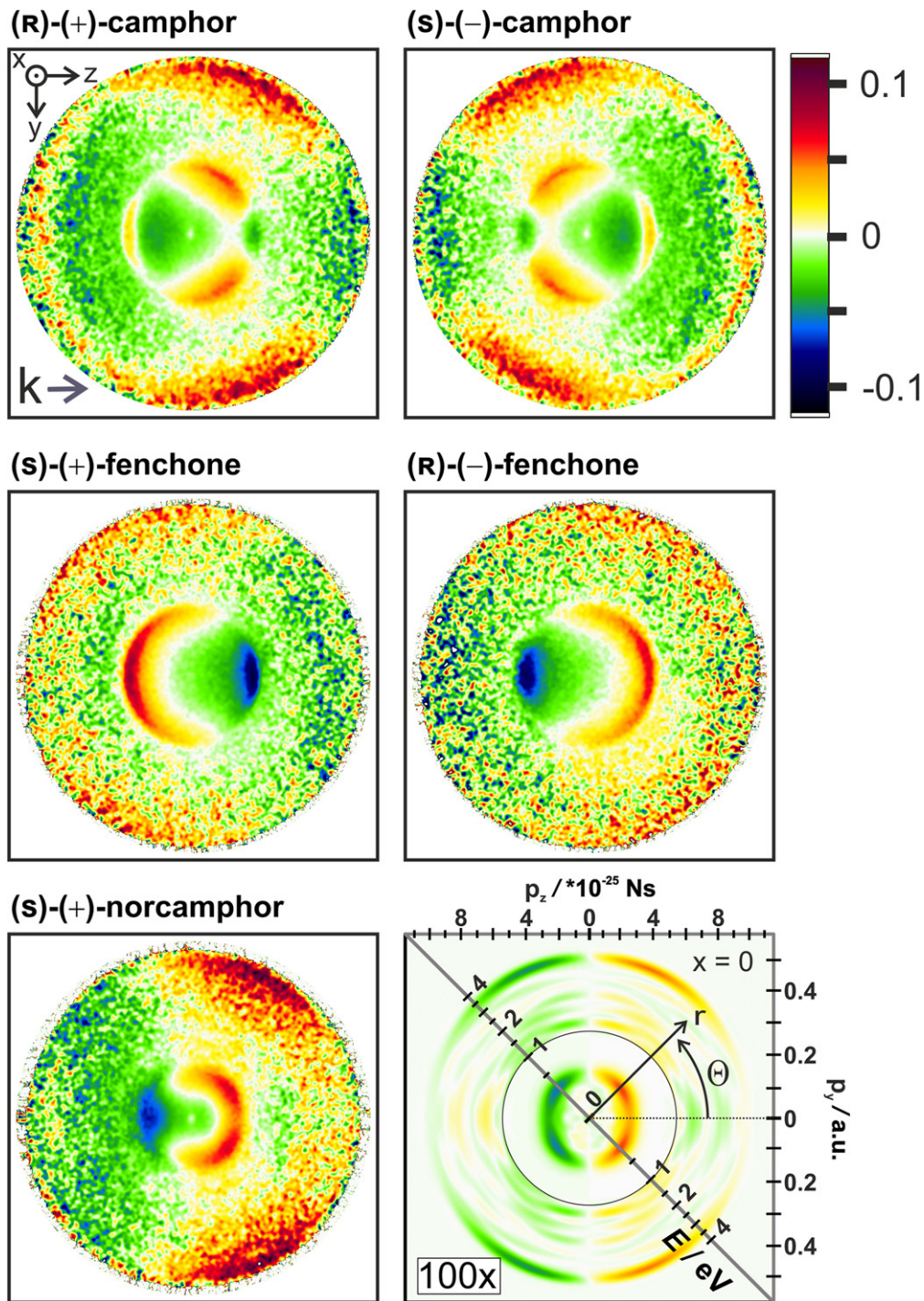


**Figure 1.** Images of the PECD contrast (see equation (3)) from the investigated bicyclic ketones (R)-(+)-camphor and (S)-(-)-camphor (upper row), (S)-(+)-fenchone and (R)-(-)-fenchone (middle row) and (S)-(+)-norcamphor (lower row, left image) obtained from measured LCP and RCP PAD-images at a peak intensity  $I_0$  of about  $1 \times 10^{13} \text{ W cm}^{-2}$ . These contrast images are displayed in an energy range up to 4 eV excess energy. Lower row, right image: Abel-inverted antisymmetric part of the PECD-image (see equation (2)) from (S)-(+)-norcamphor shown with calibrated scales of energy and momentum. The emission angle of the photoelectrons is  $\Theta$  (see equation (1)) and the radius  $r$  is proportional to the square root of the excess energy. For convenience  $p_z$  and  $p_y$  axis are given in SI units and atomic units respectively. For visualization, photoelectron signals at excess energies higher than 1 eV are increased by a factor of 100.

these coefficients represent the obtained PAD from ionization with LCP laser pulses at  $I_0$ . The Legendre coefficients are given in per cent of the respective zeroth order coefficient. This enables a comparison of both energy channels with respect to their angular distribution despite the difference in

the total signals. In the measured Abel-inverted data the threshold signal is about 30 times higher than the ATI signal (see supporting information).

For all investigated molecules a clear shift to higher orders can be recognized comparing the Legendre coefficients

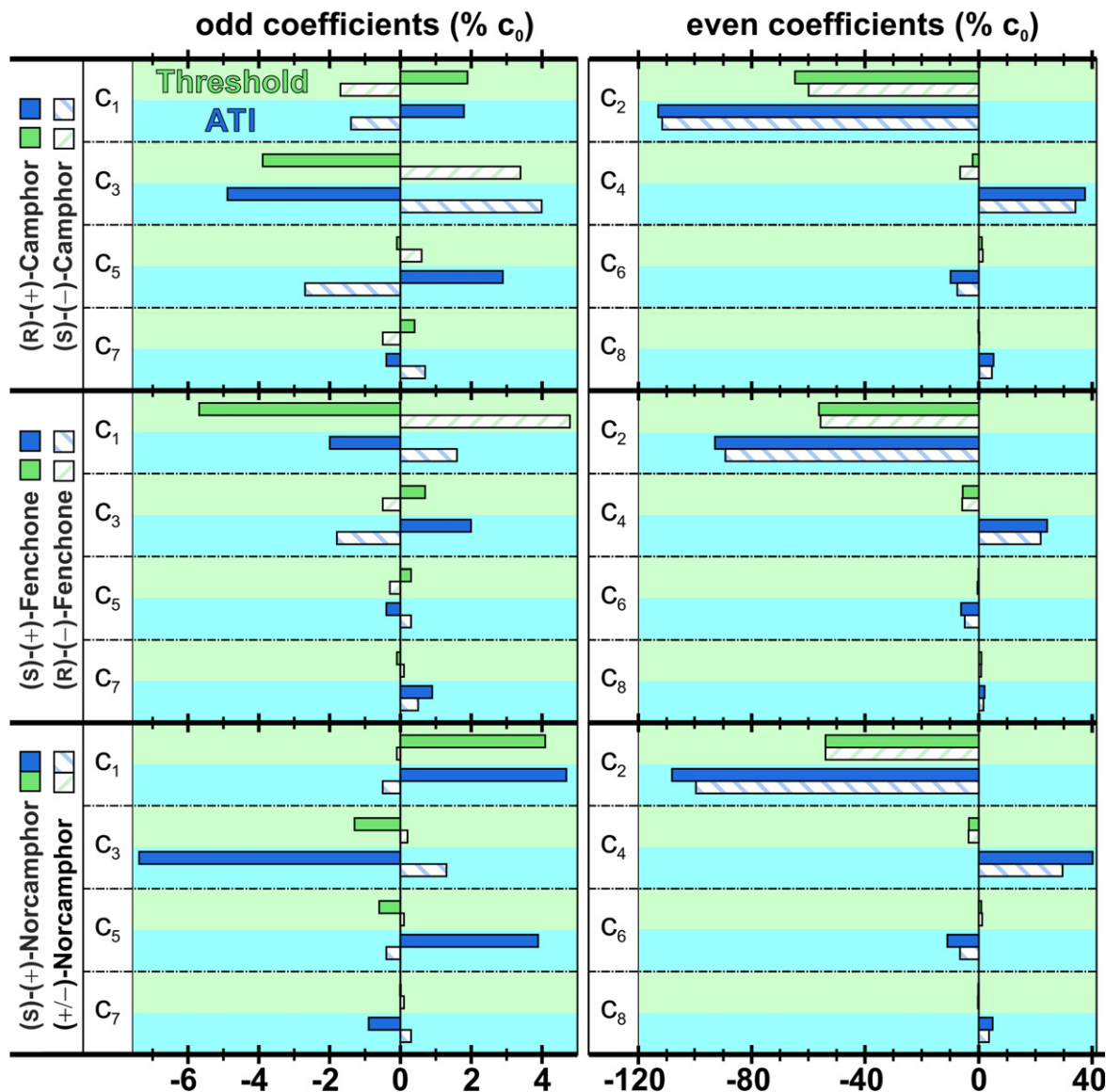


**Figure 2.** Retrieved Legendre coefficients  $c_l$  for the investigated bicyclic ketones camphor, fenchone and norcamphor. These coefficients are obtained from the Abel-inverted data within the FWHM of the energy distribution for the threshold ionization (green) and first ATI (blue). The Legendre coefficients are given in percent of the zeroth order coefficient. Different enantiomers are distinguished by solid or striped bars (see legend on the left of each row). (rac.)-(+/-)-norcamphor was measured at  $\sim 0.5 \cdot I_0$ . Numerical values for the presented coefficients are listed in the supporting information.

$c_l$  of threshold to ATI (see figure 2). High order Legendre coefficients arise up to  $l_{\max} = 2n$ . For the enantiomeric pure specimen, high odd order Legendre coefficients emerge for both energy channels and the significant coefficients change their sign on exchanging the enantiomer. In all cases the even order coefficients stay nearly unchanged (see figure 2). As a check of consistency, the almost racemic mixture of norcamphor shows only very weak amplitudes in the odd order coefficients in comparison to the almost enantiomeric pure (s)-(+)-norcamphor but nearly the same even order coefficients. Furthermore, for each enantiomer a change in sign between consecutive odd order Legendre coefficients can be observed for threshold ionization as well as for ATI. For ATI this change of sign is clearly visible on the even order Legendre polynomials, too.

For a further quantitative comparison of the PECD from the threshold contribution to the ATI contribution, we evaluate the linear PECD (LPECD). The LPECD is determined by taking twice the difference between forward and backward emission of the photoelectrons normalized to the mean intensity per hemisphere [16]. Extended to the present multiphoton case [20, 21], the LPECD—which is a one dimensional quantification of the PECD effect—can be expressed in terms of the retrieved Legendre coefficients as follows [19]:

$$\text{LPECD} = \frac{1}{c_0} \left( 2c_1 - \frac{1}{2}c_3 + \frac{1}{4}c_5 - \frac{5}{32}c_7 \right). \quad (4)$$

The derived LPECD values are listed in table 1. In the case of camphor, the retrieved LPECD values are around 5% for threshold ionization and are slightly higher in ATI (around

**Table 1.** LPECD of the investigated bicyclic ketones derived according to equation (4) within the FWHM of the threshold ionization (Thresh.) respectively above-threshold ionization (ATI).

|                              | (R)-(+)-camphor | (S)-(-)-camphor | (S)-(+)-fenchone | (R)-(-)-fenchone | (S)-(+)-norcamphor | (rac.)-(+/-)-norcamphor |
|------------------------------|-----------------|-----------------|------------------|------------------|--------------------|-------------------------|
| LPECD <sub>Thresh.</sub> (%) | 5.7             | -4.9            | -11.6            | 9.7              | 8.8                | -0.3                    |
| LPECD <sub>ATI</sub> (%)     | 6.8             | -5.5            | -5.2             | 4.1              | 14.2               | -1.7                    |

6%). Fenchone possesses a LPECD for threshold ionization of about 10% and shows weaker values for ATI, which are around 5%. The LPECD of (s)-(+)-norcamphor is approx. 9% in threshold ionization and increases to 14% in ATI. Consequently, there is no uniform trend of the LPECD between threshold ionization and ATI.

Differences in the retrieved coefficients as well as in the derived quantitative values of fenchone correlate with the different ee-values for both chemical samples. An extended study about the sensitivity of the PECD-effect with respect to the enantiomeric excess has been performed and will be published elsewhere.

Our results show a PECD-effect in threshold ionization as well as in ATI. The obtained angular distributions include high order Legendre polynomials which are related to the involved number of photons in the ionization scheme. Additionally to the expected even order Legendre polynomials also significant coefficients of the high odd order Legendre polynomials appear in the PADs from threshold ionization and ATI. A change in sign is observed for alternating even and odd coefficients. The maximum order is about two times the number of photons. Despite their similarities in chemical structure all investigated chiral molecules reveal an individual set of coefficients for the threshold and ATI signatures. The PADs and the retrieved Legendre coefficients reflect the fact that for ATI more angular momentum is absorbed than in threshold ionization. However, one-dimensional quantification via LPECD displays higher absolute values for ATI compared to threshold only in two of the studied samples. All these observations derived from a consistent data set may therefore be well suited as a benchmark for the development of theoretical approaches describing the interaction and ionization of chiral molecules with chiral light beyond the one-photon regime.

We gratefully acknowledge financial support by the State Initiative for the Development of Scientific and Economic Excellence (LOEWE) in the LOEWE-Focus ELCH and discussions with Professor Dr Robert Berger, Professor Dr Philipp Demekhin, Professor Dr Christiane Koch and Professor Dr Manfred Lein.

## References

[1] Einstein A 1905 *Ann. Phys.* **322** 132

- [2] Reid K L 2003 *Annu. Rev. Phys. Chem.* **54** 397
- [3] Reinert F and Hufner S 2005 *New J. Phys.* **7** 97
- [4] Hockett P, Wollenhaupt M, Lux C and Baumert T 2014 *Phys. Rev. Lett.* **112** 223001
- [5] Lawrence E O and Chaffee M A 1930 *Phys. Rev.* **36** 1099
- [6] Meyerand R G and Haught A F 1963 *Phys. Rev. Lett.* **11** 401
- [7] Voronov G S and Delone N B 1965 *Sov. Phys. JETP Lett.* **1** 66
- [8] Agostini P, Fabre F, Mainfray G, Petite G and Rahman N K 1979 *Phys. Rev. Lett.* **42** 1127
- [9] Humpert H J, Schwier H, Hippler R and Lutz H O 1985 *Phys. Rev. A* **32** 3787
- [10] Assion A, Baumert T, Helbing J, Seyfried V and Gerber G 1997 *Phys. Rev. A* **55** 1899
- [11] Boguslavskiy A E, Mikosch J, Gijsbertsen A, Spanner M, Patchkowskii S, Gador N, Vrakking M J J and Stolow A 2012 *Science* **335** 1336
- [12] Ritchie B 1976 *Phys. Rev. A* **13** 1411
- [13] Böwering N, Lischke T, Schmidtke B, Müller N, Khalil T and Heinzmann U 2001 *Phys. Rev. Lett.* **86** 1187
- [14] Garcia G A, Nahon L, Lebeck M, Houver J C, Doweck D and Powis I 2003 *J. Chem. Phys.* **119** 8781
- [15] Eppink A T J B and Parker D H 1997 *Rev. Sci. Instrum.* **68** 3477
- [16] Powis I 2008 *Adv. Chem. Phys.* **138** 267
- [17] Ferré A *et al* 2015 *Nat. Photonics* **9** 93
- [18] Lux C, Wollenhaupt M, Bolze T, Liang Q, Köhler J, Sarpe C and Baumert T 2012 *Angew. Chem., Int. Ed.* **51** 5001
- [19] Lux C, Wollenhaupt M, Sarpe C and Baumert T 2015 *ChemPhysChem* **16** 115
- [20] Lehmann C S, Bhargava Ram N, Powis I and Janssen M H M 2013 *J. Chem. Phys.* **139** 234307
- [21] Janssen M H M and Powis I 2014 *Phys. Chem. Chem. Phys.* **16** 856
- [22] Cooper J and Zare R N 1968 *J. Chem. Phys.* **48** 942
- [23] Yang C N 1948 *Phys. Rev.* **74** 764
- [24] Dixit S N and McKoy V 1985 *J. Chem. Phys.* **82** 3546
- [25] Barron L D 2004 *Molecular Light Scattering and Optical Activity* (Cambridge: Cambridge University Press)
- [26] Dreissigacker I and Lein M 2014 *Phys. Rev. A* **89** 53406
- [27] Artemyev A N, Müller A D, Hochstuhl D and Demekhin P V 2015 *J. Chem. Phys.* **142** 244105
- [28] Shurcliff W A 1962 *Polarized Light: Production and Use* (Cambridge, MA: Harvard University Press)
- [29] Pulm F, Schramm J, Hormes J, Grimme S and Peyerimhoff S D 1997 *Chem. Phys.* **224** 143
- [30] Freeman R R, Bucksbaum P H, Milchberg H M, Darack S, Schumacher D and Geusic M E 1987 *Phys. Rev. Lett.* **59** 1092
- [31] Garcia G A, Nahon L and Powis I 2004 *Rev. Sci. Instrum.* **75** 4989

# Supporting Information

## Photoelectron Circular Dichroism observed in the Above-Threshold Ionization Signal from Chiral Molecules with Femtosecond Laser Pulses

Christian Lux,<sup>1</sup> Arne Senftleben,<sup>1</sup> Cristian Sarpe,<sup>1</sup> Matthias Wollenhaupt<sup>2</sup>

and Thomas Baumert\*<sup>1</sup>

<sup>1</sup> *Institut für Physik und CINSaT, Universität Kassel, Heinrich-Plett-Straße 40, 34132 Kassel, Germany*

<sup>2</sup> *Institut für Physik, Carl von Ossietzky Universität Oldenburg, Carl-von-Ossietzky-Straße 9-11, 26129 Oldenburg, Germany*

TABLE SI 1. Legendre coefficients and quantification for camphor. [a] See Eq (1). [b] Corresponding Legendre coefficients of each enantiomer within the FWHM (threshold approx. 0.46 – 0.61 eV, ATI approx. 3.4 – 3.9 eV). [c] *LPECD* according to Eq. (4) (within the FWHM). For each FWHM the total signals of Threshold : ATI are 23:1.

| Legendre polynomial <sup>[a]</sup> | (R)-(+)-camphor, LCP <sup>[b]</sup> |        | (S)-(-)-camphor, LCP <sup>[b]</sup> |        | Quantification <sup>[c]</sup> |        |
|------------------------------------|-------------------------------------|--------|-------------------------------------|--------|-------------------------------|--------|
|                                    | Thresh.                             | ATI    | Thresh.                             | ATI    |                               |        |
| $c_0$                              | 1.000                               | 1.000  | 1.000                               | 1.000  |                               |        |
| $c_1$                              | 0.019                               | 0.018  | -0.017                              | -0.014 | $LPECD_{(+)\text{Thresh.}}$   | 5.7 %  |
| $c_2$                              | -0.649                              | -1.132 | -0.601                              | -1.118 | $LPECD_{(+)\text{ATI}}$       | 6.8 %  |
| $c_3$                              | -0.039                              | -0.049 | 0.034                               | 0.040  |                               |        |
| $c_4$                              | -0.022                              | 0.375  | -0.066                              | 0.341  | $LPECD_{(-)\text{Thresh.}}$   | -4.9 % |
| $c_5$                              | -0.001                              | 0.029  | 0.006                               | -0.027 | $LPECD_{(-)\text{ATI}}$       | -5.5 % |
| $c_6$                              | 0.011                               | -0.100 | 0.014                               | -0.076 |                               |        |
| $c_7$                              | 0.004                               | -0.004 | -0.005                              | 0.007  |                               |        |
| $c_8$                              | -0.002                              | 0.052  | 0.002                               | 0.044  |                               |        |



TABLE SI 2. Legendre coefficients and quantification for fenchone. [a] See Eq. (1). [b] Corresponding Legendre coefficients of each enantiomer within the FWHM (threshold approx. 0.46 – 0.63 eV, ATI approx. 3.5 – 3.9 eV). [c] *LPECD* according to Eq (4) (within the FWHM). For each FWHM the total signals of Threshold : ATI are 42:1.

| Legendre polynomial <sup>[a]</sup> | (S)-(+)-fenchone, LCP <sup>[b]</sup> |        | (R)-(-)-fenchone, LCP <sup>[b]</sup> |        | Quantification <sup>[c]</sup> |         |
|------------------------------------|--------------------------------------|--------|--------------------------------------|--------|-------------------------------|---------|
|                                    | Thresh.                              | ATI    | Thresh.                              | ATI    |                               |         |
| $c_0$                              | 1.000                                | 1.000  | 1.000                                | 1.000  |                               |         |
| $c_1$                              | -0.057                               | -0.020 | 0.048                                | 0.016  | $LPECD_{(+)\text{Thresh.}}$   | -11.6 % |
| $c_2$                              | -0.565                               | -0.932 | -0.559                               | -0.895 | $LPECD_{(+)\text{ATI}}$       | -5.2 %  |
| $c_3$                              | 0.007                                | 0.020  | -0.005                               | -0.018 |                               |         |
| $c_4$                              | -0.057                               | 0.241  | -0.059                               | 0.218  | $LPECD_{(-)\text{Thresh.}}$   | 9.7 %   |
| $c_5$                              | 0.003                                | -0.004 | -0.003                               | 0.003  | $LPECD_{(-)\text{ATI}}$       | 4.1 %   |
| $c_6$                              | -0.002                               | -0.063 | -0.005                               | -0.050 |                               |         |
| $c_7$                              | -0.001                               | 0.009  | 0.001                                | 0.005  |                               |         |
| $c_8$                              | 0.009                                | 0.020  | 0.008                                | 0.016  |                               |         |

TABLE SI 3. Legendre coefficients and quantification for norcamphor. [a] See Eq. (1). [b] Corresponding Legendre coefficients of the (+)-enantiomer and the racemic mixture within the FWHM (threshold approx. 0.18 – 0.35 eV, ATI approx. 3.2 – 3.6 eV). [c] (rac.)-(+/-)-norcamphor measured at  $\sim 0.5 \cdot I_0$ . [d] *LPECD* according to Eq. (4) (within the FWHM). For each FWHM the total signals of Threshold : ATI are 28:1.

| Legendre polynomial <sup>[a]</sup> | (S)-(+)-norcamphor, LCP <sup>[b]</sup> |        | (rac.)-(+/-)-norcamphor, LCP <sup>[b,c]</sup> |        | Quantification <sup>[d]</sup> |        |
|------------------------------------|--|--------|---|--------|-------------------------------|--------|
|                                    | Thresh.                                | ATI    | Thresh.                                       | ATI    |                               |        |
| $c_0$                              | 1.000                                  | 1.000  | 1.000   | 1.000  |                               |        |
| $c_1$                              | 0.041                                  | 0.047  | -0.001  | -0.005 | $LPECD_{(+)\text{Thresh.}}$   | 8.8 %  |
| $c_2$                              | -0.541                                 | -1.083 | -0.541  | -0.966 | $LPECD_{(+)\text{ATI}}$       | 14.2 % |
| $c_3$                              | -0.013                                 | -0.074 | 0.002   | 0.013  |                               |        |
| $c_4$                              | -0.035                                 | 0.402  | -0.036  | 0.295  | $LPECD_{(+/-)\text{Thresh.}}$ | -0.3 % |
| $c_5$                              | -0.006                                 | 0.039  | 0.001   | -0.004 | $LPECD_{(+/-)\text{ATI}}$     | -1.7 % |
| $c_6$                              | 0.009                                  | -0.111 | 0.012   | -0.066 |                               |        |
| $c_7$                              | 0.000                                  | -0.009 | 0.001   | 0.003  |                               |        |
| $c_8$                              | -0.002                                 | 0.049  | -0.003  | 0.036  |                               |        |

FIG. SI 1. Graphic representation of the observed PECD-effect in the photoelectron signal from the investigated bicyclic ketones camphor (CAM), fenchone (FEN) and norcamphor (NOR) resulting from threshold ionization and ATI with circularly polarized laser pulses at 398 nm central wavelength and a peak intensity  $I_0$ . The Abel-inverted PECD-images have been radially integrated within the FWHM of the energy channels from threshold ionization and ATI and are presented as a function of the angle  $\theta$  [see figure (a)]. For a qualitative comparison between the investigated chiral molecules and the energy channels of threshold ionization and ATI, the graphs have been normalized to the maximum of the absolute values in the PECD distribution. Different enantiomers are represented by solid and dashed lines. The energy distribution for the threshold ionization is plotted in green and the ATI in blue. Note the mirror behavior in the graphs from the antisymmetric parts when changing the handedness of the measured enantiomer. Moreover, additional nodes appear from the threshold ionization to the ATI in the graphs from the antisymmetric as well as from the symmetric parts. This behaviour in the antisymmetric parts is further illustrated in polar plots that are shown in figure (b). The sign of the function is represented by different colours and the amplitude by the radius on the curves.

